The bioelectronic neural pixel: chemical stimulation and electrical sensing at the same site

Amanda Jonsson, Sahika Inal, Ilke Uguz, Adam Williamson, Loig Kergoat, Jonathan Rivnay, Dion Khodagholy, Magnus Berggren, Christophe Bernard, George G Malliaras and Daniel T Simon

Original Publication:

Amanda Jonsson, Sahika Inal, Ilke Uguz, Adam Williamson, Loig Kergoat, Jonathan Rivnay, Dion Khodagholy, Magnus Berggren, Christophe Bernard, George G Malliaras and Daniel T Simon, The bioelectronic neural pixel: chemical stimulation and electrical sensing at the same site, 2016, Proceedings of the National Academy of Sciences of the United States of America vol 113 (issue 34): 9440-9445.
http://dx.doi.org/10.1073/pnas.1604231113

The bioelectronic neural pixel: chemical stimulation and electrical sensing at the same site

Amanda Jonsson[1]*
Sahika Inal[2]*
Ilke Uguz[2]*
Adam Williamson[3,4]*
Loïg Kergoat[1,3,4]
Jonathan Rivnay[2†]
Dion Khodagholy[2††]
Magnus Berggren[1]
Christophe Bernard[3,4]
George G. Malliaras[2]
Daniel T. Simon[1§]

[1] Laboratory of Organic Electronics, Linköping University, Department of Science and Technology, 601 74 Norrköping, Sweden
[2] Department of Bioelectronics, Ecole Nationale Supérieure des Mines, CMP-EMSE, MOC, 13541 Gardanne, France
[3] Aix Marseille Université, INS, 13005 Marseille, France
[4] Inserm, UMR_S 1106, 13005 Marseille, France

* These authors contributed equally.

† Present address: Electronic Materials and Devices Lab, Xerox PARC, 3333 Coyote Hill Road, Palo Alto, CA 94304, USA
†† Present address: NYU Neuroscience Institute, School of Medicine, New York University, New York, NY 10016, USA

§ Corresponding author: Daniel T. Simon, tel: +4611363476, email: daniel.simon@liu.se

Classification: PHYSICAL SCIENCES: Applied Physical Sciences and
BIOLOGICAL SCIENCES: Neuroscience

Abstract

Local control of neuronal activity is central to many therapeutic strategies aiming to treat neurological disorders. Arguably the best solution would make use of endogenous highly localized and specialized regulatory mechanisms of neuronal activity, and an ideal therapeutic technology should sense activity and deliver endogenous molecules at the same site for the most efficient feedback regulation. Here, we address this challenge with an organic electronic multifunctional device that is capable of chemical stimulation and electrical sensing at the same site, at the single cell scale. Conducting polymer electrodes recorded epileptiform discharges induced in mouse hippocampal preparation. The inhibitory neurotransmitter, γ-aminobutyric acid (GABA), was then actively delivered through the recording electrodes via organic electronic ion pump technology. GABA delivery stopped epileptiform activity, recorded simultaneously and colocally. This multifunctional "neural pixel" creates a range of opportunities, including implantable therapeutic devices with automated feedback, where locally recorded signals regulate local release of specific therapeutic agents.

Keywords: organic electronics, controlled delivery, electrophysiology, epilepsy, therapy

Significance statement

Electronically and ionically conducting polymers provide a unique means to translate electronic addressing signals into chemically specific and spatiotemporally resolved delivery, without fluid flow. These materials have also been shown to provide high fidelity electrophysiological recordings. Here, we demonstrate the combination of these qualities of organic electronics in multiple 20x20 μm delivery/sensing electrodes. The system is used to measure epileptic activity in a brain slice model, and deliver inhibitory neurotransmitters to the same sites as the recordings. These results represent the first time a single cell-scale electrode has had the ability to both record and chemically stimulate, demonstrating the local effects of therapeutic treatment, and opening a range of opportunities in basic neuroscience as well as medical technology development.

Introduction

Recent estimates suggest neurological disorders affect up to 6 % of the global population (1). The vast majority of treatments generally involves oral administration of pharmaceuticals. When these fail, alternate therapies can include neurosurgery (*e.g.*, in epilepsy) and electrical stimulation via implanted electrodes (*e.g.*, in Parkinson's disease (1)). Pharmaceutical and basic research have identified promising targets and designed potentially efficient drugs for multiple disorders, but such drugs haven't reached patients because of failure during (pre)-clinical tests. There are multiple reasons for such failures. Drugs may be toxic in the periphery (2, 3), they may not cross the blood brain barrier or be pumped back to the blood stream by multi-drug transporters (4, 5). But the critical factor is the fact that they may have deleterious side effects when they penetrate "healthy" regions, affecting physiological functions such as memory and learning (6, 7). In addition, since oral administration will lead to a dilution of the drug in the body, there is often a mismatch between the dose necessary to obtain a therapeutic effect in the region to treat and the maximum dose that non-affected body regions can support without side effects.

Providing the drug past the blood brain barrier, where and when it is needed, constitutes the ideal solution. Such delivery would solve all the above-mentioned problems (blood brain barrier crossing, peripheral toxicity, undesirable side effects in healthy regions and effective dose). Devices have been successfully designed to deliver drugs locally (8). However, the "where" and "when" issues remain to be addressed. Since clinicians may have several spatially distributed regions to treat, or if the volume of the intended treatment region is large, it is important to have multiple drug delivery sites, which would solve the "where" issue. The "when" issue is more difficult to address, as, ideally, a delivery system should act on-demand, when needed (*e.g.*, just before an impending seizure). Since electrophysiological signals can be used to predict incoming pathological events (9), electrical activity should be measured at each delivery site to trigger drug delivery at that specific location. Such local, real-time measurement, and precision delivery, would pave the way for closed-loop, fully automatic, therapeutic devices. Finally, since the size of the region to treat may be small – down to the scale of a single cell – the technology should allow spatial resolution of delivery on the order of micrometers.

Interfacing malfunctioning neurological pathways with spatial resolution and signal specificity approaching those of the cell could provide significant advantages to future therapies. Microelectrode recordings of the field potentials generated by neurons (or even neuronal firing itself) have become routine in investigations of brain function and dysfunction (10). Small size of recording sites allows for recording of single neurons, and densely packed sites on minimally invasive electrodes enhance the sampling capacity of the probe (11). Such densely packed probes can be accomplished using conducting polymers, such as poly(3,4-ethylenedioxythiophene) doped with poly(styrenesulfonate) (PEDOT:PSS), without decreasing the quality of the recordings. Conducting polymer electrodes exhibit inherently low impedance characteristics (more than one order of magnitude lower than bare Au, Pt and Ir electrodes of similar dimensions at 1 kHz), with the low impedance being attributed partly to the high porosity, giving an increased electrochemical surface

area (12-14). Additionally, with their mixed electronic and ionic conductivity and the soft mechanical properties that match those of the neural tissue, conducting polymers are ideally suited to obtain high signal-to-noise ratio recordings at the neural interface (15, 16). Recently, we have demonstrated microelectrode arrays based on PEDOT:PSS electrodes for *in vitro* recordings of electrophysiological signals from rat brain slices (17). These microelectrodes, fabricated at small size and high density, have enabled a good match with the dimensions of neural networks while maintaining high-resolution neural recordings.

We have also demonstrated substance delivery mimicking exocytotic release of neurotransmitters at the neuronal scale by means of the organic electronic ion pump (OEIP) (18, 19). The OEIP utilizes conducting polymer electrodes to electrophoretically "pump" neurotransmitters through a permselective membrane, enabling high spatiotemporal delivery resolution, without necessitating liquid flow. OEIPs have been utilized *in vitro* to trigger cell signaling (18, 20) and to control epileptiform activity *in vitro* (21), as well as *in vivo* to effect sensory function (19) and as a therapy for pain in awake animals (22). OEIPs have also been demonstrated in a biosensor-regulated system—on a macroscopic scale—to mimic the chemical-to-electrical-to-chemical signal transduction of neurons (23). However, none of these devices meet the desired requirement to record and deliver drugs at the same site.

In this article, we engineered a device able to perform electrical sensing of local field potentials and neurotransmitter delivery at the same site. To achieve this co-localized sensing and delivery we developed a system consisting of an array of OEIP delivery points, where each delivery point is integrated with a conducting polymer electrode for recording neuronal activity. Each integrated delivery/sensing pixel is at the single-cell scale and mimics the multifunctionality of a biological neuron: electrical information can be sensed from the local cellular environment, and neuroactive compounds can be delivered diffusively, without liquid flow, at the same location. We report on the development and characterization of this system of "neural pixels", and we demonstrate its use by delivering the endogenous inhibitory neurotransmitter γ-aminobutyric acid (GABA) to locally affect cells while simultaneously monitoring how the delivery modulates the cells' firing patterns.

Results

Design and working principle

We designed our bioelectronic neural pixel as depicted in Figure 1. The charged compound to be delivered is transported from an aqueous reservoir through a cation-conducting channel and through part of the PEDOT:PSS recording electrode before being released to the biological system. In this way, the cells close to the OEIP outlets are affected by the delivery, and the electrodes can record the subsequent modifications in cellular response. The OEIP transports cations by migration; when a potential is applied between an electrode in the reservoir and an electrode in the medium containing

the biological system under study, an electric field is established across the cation-conducting channel and a current arises from cation migration from the reservoir to the biological system. In this way, delivery is only achieved when non-zero voltage is applied (see Supplementary Information for more details on on-off switching). The cation-conducting channel has a high concentration of fixed negative charges and is therefore permeable to cations but not to anions (Donnan exclusion) (24), and is therefore a form of cation exchange membrane (CEM). Ideally, all the current passed through a CEM, and thus through the device, is due to cation transport, and no anions are transported in the opposite direction. This means that the delivery rate is directly proportional to the current, with 1 µA corresponding to a delivery rate of 10 nmol/s. Sustained delivery (constant current) requires nonpolarizable high capacity electrodes that can transfer charge between the electrode and the electrolyte. We used PEDOT:PSS electrodes for this purpose, on top of which were placed the source (reservoir) and target electrolytes (Figure 2a). Note that no potential was applied to the recording electrodes at the delivery outlets to control the delivery of ions.

Fabrication and characterization

The materials and processing of an OEIP and a conducting polymer microelectrode array (MEA) are of similar nature, making it possible to manufacture the two components of the merged device simultaneously on a single glass substrate. To fabricate the bioelectronic neural pixel device, we developed a manufacturing protocol based on standard microfabrication techniques. Device fabrication is depicted Figure 2b. First, gold electrodes were patterned on a glass substrate using photolithography and lift-off. Then the main element of the OEIP, the cation exchange membrane (CEM), made from the polyanion poly(styrene sulfonate-co-maleic acid) (PSSA-co-MA) cross-linked with poly(ethylene glycol) (PEG), was deposited. The CEM was photolithographically patterned and dry-etched into a wide channel leading to 32 thinner (and thus higher ionic resistance (22)) parallel channels ending in 20 µm-wide delivery outlets (Figure S1). Alternatively, the PSS-co-MA/PEG was patterned by peel-off using parylene (see Methods section). A 2 µm-thick parylene layer, providing the insulating coating of the OEIP and the MEA contacts, was deposited. A thin layer of dilute commercial cleaner was applied as an anti-adhesive coating and a second 2 µm-thick parylene layer was deposited. Openings to define the OEIP electrolytes, the microelectrodes, and the contact pads were obtained by further photolithography and plasma etching through the parylene. PEDOT:PSS was then deposited by spin-coating, and the second parylene layer was peeled off to define the OEIP electrolytes and the microelectrodes. The 32 resulting neural pixels thus comprised 20x20 µm PEDOT:PSS recording electrodes at the delivery end of each PSSA-co-MA-based OEIP channel. In this way, substance delivery was achieved *through* the PEDOT:PSS recording electrode, such that the delivery outlet and the recording electrode were indeed at the same site (Figure 1). Finally, a PDMS gasket was cut with openings over the source electrodes, defined the source solution well, and over the 32 neural pixels and target electrode, defining the target solution well (Figure S2).

To characterize the multifunctional device, we first measured the impedance of the recording electrodes separately, and then while running a delivery current through the OEIP to investigate whether running the delivery current through the recording electrodes affected the electrical

properties of the recording electrodes. The Bode plot of the mean impedance magnitude of seven randomly picked PEDOT:PSS electrodes of the array is presented in Figure 3a. The standard deviation of the impedance magnitude is low, indicating that the fabrication process yielded homogeneous electrode properties within the array. Between 10 kHz and 10 Hz the impedance increased from 16 kΩ to 250 kΩ, and at 1 kHz, the impedance was ca. 19 kΩ, which is similar to our previously reported results (17).

To further investigate the influence of OEIP operation on the signal to noise ratio, we compared electrode recordings in the absence and presence of a delivery current (Figure 3b). A 100 mM GABA(aq) solution and artificial cerebrospinal fluid (ACSF) were placed on the source and the target side, respectively. The amplitude of the baseline signal measured when the OEIP was off was ca. 10 µV (Figure 3b). After 60 s, a positive potential was applied to the OEIP source electrode with respect to the target, and a current of 1 µA was run through the device, yielding GABA delivery at the 32 outlets. The electrical signal intensity recorded remained stable. The OEIP was switched off after 60 s without apparent change in signal amplitude. A too high delivery rate could affect the recording electrodes by perturbing the local ion concentration, making cell recordings difficult or impossible. However, as seen in this experiment, constant currents of 1 µA or lower are compatible with electrophysiological recordings.

In vitro validation with complete hippocampus preparations – inhibiting epileptiform activity

After confirming that cation delivery did not interfere with electrode recordings, we evaluated sensing and stimulation performance of the pixels in a biological system. As the first application of the integrated device could be for epilepsy diagnosis and treatment, we used complete extracted hippocampus preparations from mouse (P7-P12) and triggered epileptiform activity by pharmacological manipulation, namely the addition of 4-aminopyridine (4-AP) to the perfusion. 4-AP is a selective blocker of channels belonging to the Kv1 family of voltage-gated K^+ channels. Blocking K^+ channels with 4-AP in the perfusion produces epileptiform activity by increasing the time required for a neuron to repolarize (fewer K^+ channels are available). Thus, neurons remain above the threshold to fire for a longer period of time, and excitatory neurons consequently continue to deliver glutamate to downstream neighbors.

In order to test the efficacy of the device, we chose to deliver GABA. As an endogenous neurotransmitter, GABA activates $GABA_A$ receptors, leading to Cl^- influx into the cell, which in turn hyperpolarizes the cell membrane (Figure 4a). In addition, the opening of these channels decreases the membrane resistance, creating a shunt effect, and limiting the effectiveness of excitatory inputs. The net effect of GABA is therefore a decrease in the firing probability of the cell (25).

With the complete extracted hippocampus preparation mounted (and equilibrated) on the target area of the neural pixel system, we induced epileptiform activity with the addition of 4-AP in the perfusion medium. PEDOT:PSS electrodes recorded the subsequent broadband electrophysiological activity (Figure 4b). The recordings, which were simultaneously obtained via multiple channels, had signal quality comparable to a conventional tungsten recording electrode, which was located adjacent to the MEA (Figure S3). Moreover, due to multiple recording sites, it is possible to access different forms of activity across the tissue. After ca. one minute of GABA delivery, epileptiform discharges were abolished. Assuming that the delivery is equally distributed between the 32 outlets of the device, 1 µA of supply current yields a delivery rate of 0.3 pmol.s^{-1}.$outlet^{-1}$. This corresponds to a local concentration change of 25 µM at distance of 400 µm from a single pump outlet (18, 21) after 60 s, and is within the known range for GABA to suppress hyperactivity (26) (injection of 250 µM GABA in the ACSF-filled bath directly on top of the tissue stopped the hyperactivity almost instantaneously (Figure S4)). Previous experiments demonstrated local delivery with OEIPs (Ref. (22) and Figure S5), and local control of hippocampal networks with a similar device geometry (21). Taken together, these results demonstrate that the neural pixel system can effectively control the activity of a given network via OEIP delivery, while simultaneously allowing monitoring via the integrated electrodes of both hyperactivity as well as real-time biological response to OEIP operation.

Since GABA is an acid and is transported by the OEIP in its fully protonated form (charge +1), each GABA molecule will release a proton once delivered to the biological system. Therefore, to verify that the observed abolishment of of epileptiform discharges was solely due to GABA delivery, and not to proton delivery, or to the applied potentials and ionic currents, a control experiment delivering protons was performed. The reservoir was filled with aqueous HCl solution, while the target region contained the hippocampus exhibiting hyperactivity. The same current was sourced to the OEIP as for the GABA delivery experiments, however we did not observe any significant change in the electrode recordings upon delivery of H^+ (Figure 4c). This shows that neither proton delivery nor ionic currents (which could cause electrical stimulation) blocked the pathological activity, but that the release of GABA was necessary to to stop epileptiform activity.

Discussion

In the present work, we have demonstrated electrophysiological sensing and chemical stimulation from a single multifunctional “neural pixel”. This is a necessary advancement to achieve highly localized feedback-regulated therapies with future devices. We have previously shown that we could deliver GABA with an OEIP to stop epileptiform activity in a tissue slice (21). In those experiments, the recording electrode was a tungsten electrode positioned in the tissue slice in the vicinity of an OEIP outlet. In this work, we suppress the need to align this external recording electrode with the outlets of the OEIP. Instead, delivery occurs *through* the sensing electrodes, ensuring co-localization of recording and stimulation and eliminating cumbersome experimental setup. The integrated sensing and delivery device stopped externally induced epileptiform activity of a hippocampus by delivering the inhibitory neurotransmitter GABA at the exact sites where epileptic activity was

recorded. The low impedance of the conducting polymer electrodes allowed for high signal-to-noise ratio recordings of physiological activity at the site of GABA delivery. In order to efficiently treat an epileptic event, the delivery of GABA should occur as soon as any signs of seizure appear.

Many studies have shown local release of compounds using microfluidics, for example Refs. (27-29), to name a few. Microfluidics have the ability ot deliver any soluble compound, but such delivery in a carrier fluid induces convection, which risks disrupting fragile biochemical microenvironments . Microfluidic systems also typically require complex setups of valves and pumps. Other groups have demonstrated electrically controlled convection-free delivery systems, for example Refs. (16, 30), that rely on redox-switching of conducting polymers to release an embedded compounds. However, these systems are typically limited in the amount of deliverable compound, a release rate that decreases over time, and a poor on-off ratio. The OEIP-based delivery built into the neural pixel system is electrically controlled, induces no convection, includes a reservoir to increase the deliverable amount, and exhibits a low diffusive off-leakage because of the relatively large distance between the reservoir and the delivery points (see Supplementary Information).

While the electrical signals that turn on the OEIP can be initiated nearly instantaneously, the time required to stop the epileptiform activity after starting GABA delivery was about 60 s. For some applications, this speed may need to be significantly faster. OEIP dynamics are largely governed by the length that ions much traverse from the source electrolyte to the delivery points. In the present geometry, this length is on the scale of several millimeters. We are thus developing devices with significantly faster turn-on by arranging delivery vertically through a thin CEM film, thereby reducing the effective ion path-length to hundreds of nanometers. Likewise, the pixel dimensions in the device described above were 20x20 μm, with the 32-electrode array spanning several hundred microns. This is already on the approximate scale of single neurons, and local neuronal circuits, respectively. While miniaturization is feasible (though difficult), increasing these dimensions to fit different therapeutic targets is also possible.

Another limitation with the present neural pixel system is that it delivers ions simultaneously at the 32 outlets, where each outlet is co-localized with a sensing electrode. An addressable pixel array, where each sensing/delivery site could be individually controlled, would thus be a significant improvement. Such a system would make it possible to record from an array of electrodes, and then to selectively turn on the delivery at the sites where, for example, epileptiform activity is recorded. A future device, with individually addressable release sites and co-localized recording electrodes, could also be used as an *in vitro* tool to precisely quantify the kinetics of specific neurochemical signaling. Furthermore, such individually addressed neural pixels could enable multiple connections to a single neuron, similar to the way biological neurons connect with each other. In this way, the dynamics of multiple neural connections could be studied with unprecedented detail.

The lifetime of our device depends on the electrochemical capacity of the electrodes and the delivery rate required for the application. For an *in vitro* study like the one above, lasting only hours,

electrode capacity is not an issue, especially since consumed electrodes can easily be replaced by fresh, free-standing electrodes dipped into the electrolytes. For an implantable *in vivo* device, however, electrode capacity is crucial. Larger, or more 3D-structured electrodes and delivery in short pulses would increase the lifetime. Another solution would be to incorporate an ion diode-based current rectifier, so that the electrodes could be electrochemically "recycled", increasing the lifetime substantially (31). Likewise, for *in vivo* applications, the device could be built on flexible substrates, *e.g.,* parylene-C and wrapped onto a tissue, but additional fabrication issues such as long-term mechanical and lamination stability must also be considered. This is something we have not yet explored, however. For applications deeper inside the tissue or organ of interest, neural pixel systems could be constructed into implantable probes, a technique already demonstrated for basic OEIPs (19, 22).

The ability to sense electrophysiological signals and deliver neuroactive compounds at the same location represents a first step in constructing closed-loop feedback system, capable of monitoring neuronal activity and adjusting local release of neurotransmitters accordingly. Indeed, the system presented above only requires minor modification to the control software to explore this functionality, and we are currently engaged in these experiments. Such a closed-loop system could be used, for example, in epilepsy treatment, to predict or detect an epileptic seizure at an early stage and intervene by delivering inhibitory neurotransmitters. The feedback system would make it possible to stop seizures with a minimal amount of drugs, since the drug release could be stopped as soon as the inhibitory effect is observed.

Methods

Device fabrication. 3x1 inch diameter glass slides were cleaned by sonication in soap/water mixture and acetone/IPA mixture. For patterning gold, a photoresist, S1813 (Shipley), was spin-cast on the glass slide, exposed to UV light using a SUSS MJB4 contact aligner, and developed using MF-26 developer. Titanium and gold (100 nm) were evaporated (Alliance Concept EVA450) and patterned using lift-off in acetone. On top of a layer cast from soap/water solution, a 1.5 µm of parylene C was deposited using an SCS Labcoater 2. A 4µm of photoresist, AZ9260 was then patterned and etched (300 W, 50 sccm O_2, 5 min) using Oxford 80 plus. A solution of 3-glycidoxypropyltrimethoxysilane (GOPS, 5 wt%) in a water:ethanol mixture (1:19) was spin coated to improve the adhesion of the PSSA-co-MA on glass. After 15 min, the substrates were rinsed in ethanol to remove excess GOPS. Then the substrates were baked at 110 °C for 20 min. PSSA-co-MA (5 wt% in a water:1-propanol mixture, 1:1) was mixed with polyethylene glycol (3 wt%, molecular weight 400 $g.mol^{-1}$) for crosslinking, and then deposited by spin casting at 2000 rpm to obtain a thickness of 300 nm. The film was baked at 110 °C for 1 h. The sacrificial parylene C layer was peeled off to complete the patterning of PSSA-co-MA. Another layer of parylene‑C was deposited, reaching a final thickness of 2 µm, with the use of an adhesion promoting silane. A soap solution (1 wt% in water) was spun and followed by a subsequent parylene‑C deposition (2 µm). Finally, the source/target PEDOT:PSS was patterned with the insulating parylene‑C using photolithography and a sacrificial peel‑off step. A

thick layer of AZ9260 (MicroChemicals) photoresist was cast, baked and exposed using a SUSS MJB4 contact aligner, followed by reactive ion etching in an O_2 plasma (160 W, 50 sccm O_2, 15 min) using an Oxford 80 plus plasma etcher. For the preparation of the PEDOT:PSS films, 19 ml of aqueous dispersion (PH 1000 from H.C. Stark) was mixed with 1 ml of ethylene glycol, 50 µl of dodecyl benzene sulfonic acid and 1 wt % of GOPS, and the resulting dispersion was spin‑coated at 650 rpm, soft baked at 100°C for 60 s, and spun cast at 650 rpm to attain thicker PEDOT:PSS films. The film is patterned by peel‑off of the top parylene C film and subsequently baked at 140 °C for 1 h and were immersed in deionized water to remove any excess low molecular weight compounds. The reservoir chambers, cut from cured polydimethylsiloxane, were affixed to the source (reservoir) and target (bath) areas.

Device characterization. Impedance spectra of the electrodes were measured using an Autolab potentiostat equipped with an FRA module. Commercially available Ag/AgCl and Pt electrodes were used as the counter and reference electrodes. The applied voltage was 0.01 V and the electrolyte solution was aqueous 0.1 M NaCl(aq). The contacts of the OEIP were connected to a Keithley 2400 source/measure unit, and constant current (1 µA or lower) was sourced and voltage was measured using a customized LabVIEW software. Electrode recordings were obtained using a commercially available voltage recording setup, RHD2000 Evaluation System. As the reference electrode, a grounded Ag/AgCl electrode was immersed into the target electrolyte. The recordings were acquired at 20 kHz sampling rate and analyzed using Matlab (Mathworks)-based software with a low-pass filter of 1 kHz and down-sampled by 500.

Electrical recording data acquisition. Electrode recordings were obtained using a commercially available voltage recording setup, RHD2000 Evaluation System (Intan Technologies) (Figure S2). A 3D printed sample holder was fabricated, containing gold-coated pins in contact with the 32 gold electrode pads of the device. As the reference electrode, a grounded Ag/AgCl electrode was immersed into the target reservoir containing the brain slice. Recordings were acquired at 20 kHz sampling rate and analyzed using MATLAB (Mathworks)-based software with a low-pass filter of 1 kHz and down-sampled by 500.

Hippocampus preparation. All protocols have been approved by the Institutional Animal Care and Use Committee of INSERM. All experiments were repeated twice on different biological samples. After decapitation of anesthetized mice, brains were rapidly extracted (postnatal day 14 to 18). In a chilled and perfused bath, the brain was cut into the left and right hemisphere, and the complete hippocampus including the septum was extracted from each hemisphere. This preparation maintains the whole 3D hippocampal architecture, preserving cellular and axonal integrity (32, 33). Freshly-extracted preparations were placed in a chamber and perfused with oxygenated (95% O_2/ 5% CO_2) artificial cerebrospinal fluid (ACSF) (126 mM NaCl, 3.5 mM KCl, 2mM $CaCl_2$, 1.3 mM $MgCl_2$, 1.2mM NaH_2PO_4, 26.2 mM $NaHCO_3$, and 10 mM glucose). They were maintained in the chamber at room temperature and allowed to recover for one hour prior to experimental use. After this period of recovery, preparations were transferred with a pipette to the surface of the integrated

sensing/delivery device. The chamber containing the hippocampus was continuously perfused with oxygenated ACSF warmed at 33 °C. Tungsten electrodes (with a tip resistance of 1-3 MΩ) were positioned on top the OEIP outlets/ electrode openings. External electrode recordings were made with a World Precision Instruments DAM80 AC amplifier, and acquired using an analog-to-digital converter (Digidata 1322B, Molecular Devices). Analysis was performed using using Clampfit (Molecular Devices) or Matlab (Mathworks)-based software.

Acknowledgements

The research leading to these results has received funding from the European Union's Seventh Framework Programme (FP7/2007-2013) under grant agreement no602102 (EPITARGET) and A*MIDEX project MIDOE (A_M-AAP-ID-13-24-130531-16.31-BERNARD-HLS). Funding was also provided by the Swedish Innovation Office (VINNOVA, 2010-00507), the Swedish Research Council (Vetenskapsrådet, 621-2011-3517), and the Knut and Alice Wallenberg Foundation (KAW Scholar, 2012.0302). The authors would additionally like to acknowledge the National Science Foundation grant DMR-1105253 for partial support of this work, the ANR through the project PolyProbe (ANR-13-BSV5-0019-01), Fondation pour la Recherche Médicale under grant agreements DBS20131128446 and ARF20150934124, Fondation de l'Avenir, the Önnesjö Foundation, the Region PACA, and Microvitae Technologies. JR and LK acknowledge support from Marie Curie Fellowships. The fabrication of the device was performed in part at the Centre Microelectronique de Provence (CMP). The authors thank Gaelle Rondeau and the staff of the clean room in CMP for technical support during fabrication.

Author contributions

GGM, MB, and DTS conceived the device and experiment, with the help of DK and JR. AJ, SI, IU LK, and DTS designed the device and/or developed fabrication processes. AW and CB designed the bioexperiments. AJ, LK, SI and IU fabricated and characterized the device. AW performed the bioexperiments, SI, IU, and in some cases AJ, assisted. A.J, LK, DTS, AW and SI wrote the manuscript.

References

1. Kringelbach ML, Jenkinson N, Owen SLF, Aziz TZ (2007) Translational principles of deep brain stimulation. *Nat Rev Neurosci* 8(8):623–635.

2. Rogawski MA, Löscher W (2004) The neurobiology of antiepileptic drugs. *Nat Rev Neurosci* 5(7):553–564.

3. Bialer M, White HS (2010) Key factors in the discovery and development of new antiepileptic drugs. *Nat Rev Drug Discov* 9(1):68–82.

4. Löscher W, Potschka H (2005) Drug resistance in brain diseases and the role of drug efflux transporters. *Nat Rev Neurosci* 6(8):591–602.

5. Higgins CF (2007) Multiple molecular mechanisms for multidrug resistance transporters. *Nature* 446(7137):749–757.

6. Kwan P, Brodie MJ (2001) Neuropsychological effects of epilepsy and antiepileptic drugs. *The Lancet* 357(9251):216–222.

7. Perucca P, Gilliam FG (2012) Adverse effects of antiepileptic drugs. *The Lancet Neurology* 11(9):792–802.

8. Wolinsky JB, Colson YL, Grinstaff MW (2012) Local drug delivery strategies for cancer treatment: Gels, nanoparticles, polymeric films, rods, and wafers. *Journal of Controlled Release* 159(1):14–26.

9. Cook MJ, et al. (2013) Prediction of seizure likelihood with a long-term, implanted seizure advisory system in patients with drug-resistant epilepsy: a first-in-man study. *The Lancet Neurology* 12(6):563–571.

10. Cogan SF (2008) Neural Stimulation and Recording Electrodes. *Annu Rev Biomed Eng* 10(1):275–309.

11. Buzsáki G, Anastassiou CA, Koch C (2012) The origin of extracellular fields and currents — EEG, ECoG, LFP and spikes. *Nat Rev Neurosci* 13(6):407–420.

12. Ludwig KA, Uram JD, Yang J, Martin DC, Kipke DR (2006) Chronic neural recordings using silicon microelectrode arrays electrochemically deposited with a poly(3,4-ethylenedioxythiophene) (PEDOT) film. *Journal of Neural Engineering* 3(1):59–70.

13. Ludwig KA, et al. (2011) Poly(3,4-ethylenedioxythiophene) (PEDOT) polymer coatings facilitate smaller neural recording electrodes. *Journal of Neural Engineering* 8(1):014001.

14. Venkatraman S, et al. In Vitro and In Vivo Evaluation of PEDOT Microelectrodes for Neural Stimulation and Recording. *IEEE Trans Neural Syst Rehabil Eng* 19(3):307–316.

15. Green R, Lovell N, Wallace G, Poole-Warren L (2008) Conducting polymers for neural interfaces: Challenges in developing an effective long-term implant. *Biomaterials* 29(24-25):3393–3399.

16. Abidian MR, Kim D-H, Martin DC (2006) Conducting-Polymer Nanotubes for Controlled Drug Release. *Adv Mater* 18(4):405–409.

17. Sessolo M, et al. (2013) Easy-to-Fabricate Conducting Polymer Microelectrode Arrays. *Adv Mater* 25(15):2135–2139.

18. Tybrandt K, et al. (2009) Translating Electronic Currents to Precise Acetylcholine-Induced Neuronal Signaling Using an Organic Electrophoretic Delivery Device. *Adv Mater* 21(44):4442–4446.

19. Simon DT, et al. (2009) Organic electronics for precise delivery of neurotransmitters to modulate mammalian sensory function. *Nat Mater* 8(9):742–746.

20. Isaksson J, et al. (2007) Electronic control of Ca^{2+} signalling in neuronal cells using an organic electronic ion pump. *Nat Mater* 6:673–679.

21. Williamson A, et al. (2015) Controlling Epileptiform Activity with Organic Electronic Ion

Pumps. *Adv Mater* 27(20):3138–3144.

22. Jonsson A, et al. (2015) Therapy using implanted organic bioelectronics. *Sci Adv* 1(4):e1500039.

23. Simon DT, et al. (2015) An organic electronic biomimetic neuron enables auto-regulated neuromodulation. *Biosensors and Bioelectronic* 71(0):359–364.

24. Strathmann H (2004) *Ion-exchange membrane separation processes* (Elsevier) Available at: https://www.elsevier.com/books/ion-exchange-membrane-separation-processes/strathmann/978-0-444-50236-0.

25. Jones R (2012) Neurotransmission: GABA calls stop in the striatum. *Nat Rev Neurosci* 13(12):815–815.

26. Jones MV, Westbrook GL (1995) Desensitized states prolong GABAA channel responses to brief agonist pulses. *Neuron* 15(1):181–191.

27. Hendricks J, Chikar J, Crumling M, Raphael Y, Martin DC (2008) Localized cell and drug delivery for auditory prostheses. *Hearing Research* 242(1-2):117–131.

28. Jeong J-W, et al. (2015) Wireless Optofluidic Systems for Programmable In Vivo Pharmacology and Optogenetics. *Cell*:1–14.

29. Minev IR, et al. (2015) Electronic dura mater for long-term multimodal neural interfaces. *Science* 347(6218):159–163.

30. Svirskis D, Travas-Sejdic J, Rodgers A, Garg S (2010) Electrochemically controlled drug delivery based on intrinsically conducting polymers. *Journal of Controlled Release* 146(1):6–15.

31. Gabrielsson EO, Janson P, Tybrandt K, Simon DT, Berggren M (2014) A Four-Diode Full-Wave Ionic Current Rectifier Based on Bipolar Membranes: Overcoming the Limit of Electrode Capacity. *Adv Mater* 26(30):5143–5147.

32. Khalilov I, et al. (1997) A Novel In Vitro Preparation: the Intact Hippocampal Formation. *Neuron* 19(4):743–749.

33. Davies ML, Kirov SA, Andrew RD (2007) Whole isolated neocortical and hippocampal preparations and their use in imaging studies. *J Neurosci Meth* 166(2):203–216.

Figures

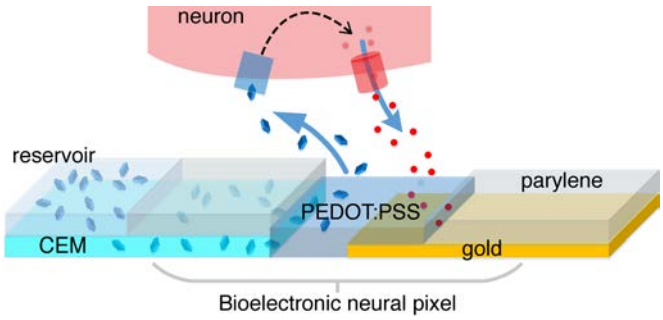

Figure 1. **The bioelectronic neural pixel**. The OEIP channel outlet (terminating in the PEDOT:PSS) co-localized with the PEDOT:PSS recording electrode forms one neural pixel. The reservoir (left) comprises an aqueous solution of the positively charged compound to be delivered through the cation exchange membrane (CEM) and out through the PEDOT:PSS recording electrode to the neural tissue above the pixel. The biological response, in terms of ion fluxes, is measured locally by the PEDOT:PSS recording electrode co-localized with the OEIP outlet.

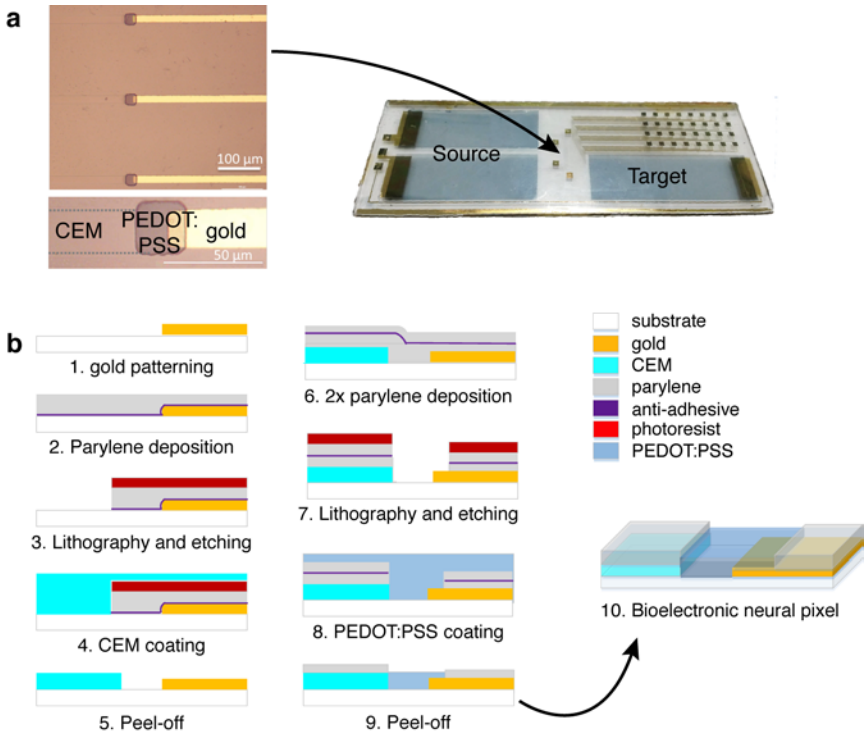

Figure 2. **Design and fabrication of the bioelectronic neural pixel.** *(a)* Microscope image of the three adjacent co-localized OEIP outlets and sensing electrodes, and photograph of a typical device. Two source electrodes are depicted, used at equipotential and thus forming effectively one electrode. The reservoir chamber, cut from cured polydimethylsiloxane (PDMS), is affixed to the source and target areas. The source contains the cation solution to be delivered, and the neural tissue is placed on the target region. Supplementary Figure S1 shows the design in more detail. *(b)* Cross-section schematics showing the photolithographic fabrication process. Gold lines were patterned with photolithography *(1)*, followed by coating of parylene-C with a thin layer of anti-adhesive *(2)*. Photoresist was then cast and exposed, followed by reactive ion etching to define the areas to be filled with CEM *(3)*. The CEM (PSSA-co-MA cross-linked with poly(ethylene glycol)) was patterned into a wide channel that split into 32 separate outlets, each 20 µm wide and spaced by 200 µm (Supplementary Figure S1) by peeling off the sacrificial top layer of parylene-C *(4, 5)*. Two layers of parylene-C were then deposited, separated by a thin layer of anti-adhesive *(6)*. A thick layer of photoresist was then cast, exposed and etched in order to define the areas eventually to be filled with PEDOT:PSS *(7)*. A thick layer of PEDOT:PSS (ca. 400 nm) was spin-cast *(8)* and the source/target electrodes and the sensing electrodes at the pump outlets were patterned by peeling off the sacrificial top layer of parylene-C *(9)*. The co-localization of an OEIP outlet with the PEDOT:PSS electrode form a neural pixel *(10)*.

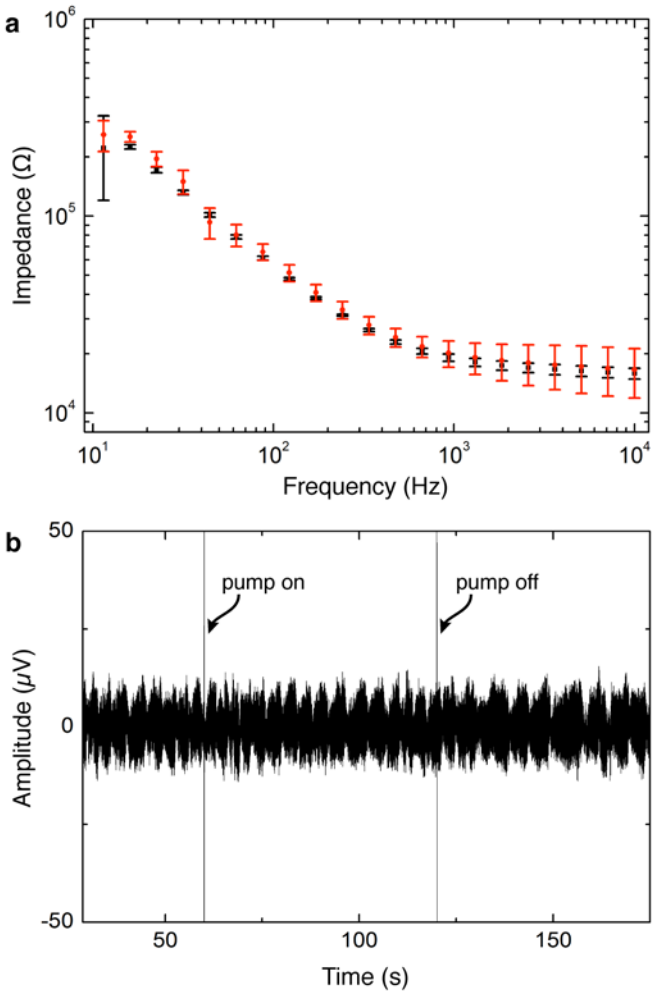

Figure 3. **Characterization of sensing electrodes incorporated into neural pixels**. *(a)* Bode plot of impedance versus frequency. The impedance magnitude is an average of seven electrodes. Black squares and red dots are the averaged impedance values while the OEIP is off and the while K^+ is delivered (1 µA delivery current), respectively. *(b)* Time trace at a single recording site during GABA delivery ($60 < t < 120$ s) through the sensing electrode to the ACSF target solution.

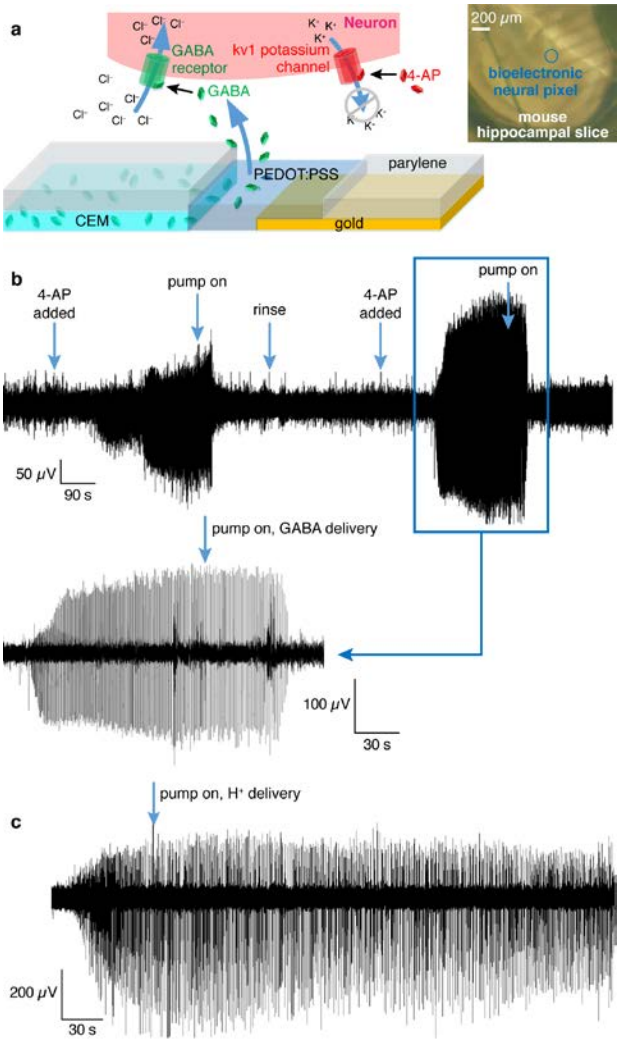

Figure 4. **Epileptiform activity simultaneously recorded and inhibited by a single neural pixel**. *(a)* Biochemical pathway for reducing 4-AP-induced epileptiform activity via GABA delivery. The inset shows a mouse hippocampal slice positioned on an array of bioelectronic neural pixels. *(b)* Epileptiform activity of a complete mouse hippocampal preparation was recorded from a single pixel before and during GABA delivery to the same pixel. Large events are seen at the beginning of the recording approximately 100 s after introducing 4-AP to the bath. Approximately 60 s after the OEIP is switched on, the epileptiform activity stops. This cycle is repeated twice by rinsing the bath with ACSF and treating the tissue with 4-AP. *(c)* Response of recording electrodes to delivery of H^+. H^+ delivery has no observable effect on epileptiform activity. The recorded signal is from the epileptic mouse hippocampal neurons upon delivery of H^+ from the OEIP outlets. The activity does not stop when the source reservoir contains HCl and ion pump is operated under the same conditions as with GABA delivery experiment. *(c)* Negative control: delivery of H^+ only. Epileptiform activity was not observed to change.